Protein Science (2000), *9*:1847–1851. Cambridge University Press. Printed in the USA.

FOR THE RECORD

Structure of streptococcal pyrogenic exotoxin A reveals a novel metal cluster

CATHLEEN A. EARHART,[1] GREGORY M. VATH,[1] MANUELA ROGGIANI,[2] PATRICK M. SCHLIEVERT,[2] AND DOUGLAS H. OHLENDORF[1]

[1]Department of Biochemistry, University of Minnesota Medical School, 6-155 Jackson Hall, 321 Church Street, SE, Minneapolis, Minnesota 55455
[2]Department of Microbiology, University of Minnesota Medical School, Box 196 UMHC, Minneapolis, Minnesota 55455

(RECEIVED April 5, 2000; FINAL REVISION June 30, 2000; ACCEPTED July 7, 2000)

Abstract: The streptococcal pyrogenic toxins A, B, and C (SPEA, SPEB, and SPEC) are responsible for the fever, rash, and other toxicities associated with scarlet fever and streptococcal toxic shock syndrome. This role, together with the ubiquity of diseases caused by *Streptococcus pyogenes*, have prompted structural analyses of SPEA by several groups. Papageorgiou et al. (1999) have recently reported the structure of SPEA crystallized in the absence of zinc. Zinc has been shown to be important in the ability of some staphylococcal and streptococcal toxins to stimulate proliferation of $CD4^+$ T-cells. Since cadmium is more electron dense than zinc and typically binds interchangeably, we grew crystals in the presence of 10 mM $CdCl_2$. Crystals have been obtained in three space groups, and the structure in the $P2_12_12_1$ crystal form has been refined to 1.9 Å resolution. The structural analysis revealed an identical tetramer as well as a novel tetrahedral cluster of cadmium in all three crystal forms on a disulfide loop encompassing residues 87–98. No cadmium was bound at the site homologous to the zinc site in staphylococcal enterotoxins C (SECs) despite the high structural homology between SPEA and SECs. Subsequent soaking of crystals grown in the presence of cadmium in 10 mM $ZnCl_2$ showed that zinc binds in this site (indicating it can discriminate between zinc and cadmium ions) using the three ligands (Asp77, His106, and His110) homologous to the SECs plus a fourth ligand (Glu33).

Keywords: cadmium; metal cluster; metal selectivity; *Streptococcus pyogenes*; superantigens; toxin; zinc

Staphylococcus aureus and group A streptococci are responsible for a number of important human diseases ranging from food poisoning to staphylococcal scalded skin syndrome, and toxic shock syndrome (TSS). TSS is a severe multisystem disorder characterized by fever, hypotension (shock), an erythematous rash, and sometimes vomiting, diarrhea, and reddening of mucous membranes. In these conditions, the infecting organisms produce a number of protein virulence factors such as proteases, nucleases, lipases, and exotoxins. Several of these exotoxins have been identified and characterized in staphylococci and streptococci. In *S. aureus*, enterotoxins types A through L excluding F (SEA-SEG, SEH-SEL) and toxic shock syndrome toxin 1 (TSST-1) have been found. In *Streptococcus pyogenes*, exotoxins type A through J excluding D, E, and I (SPEA-SPEC, SPEF-SPEH, and SPEJ), streptococcal superantigen (SSA), and streptococcal mitogenic exotoxins (SMEZ and SMEZ-2) have been identified. Collectively, these toxins are known as the pyrogenic toxin superantigens (PTSAgs). These exotoxins are so named because of their ability to bind to class II major histocompatibility complexes (MHCs) on antigen-presenting cells and T cell receptors (TCRs) on T-lymphocytes resulting in their proliferation. Unlike a conventional antigenic response where specificity resides in several complementary determining regions on the TCR, this *superantigenic* response depends only on the variable region of the TCR β-chain. These exotoxins also induce fever in their hosts (*pyrogenicity*), cause *capillary leakage* (leading to hypotension) through cytokine release, and enhance the *lethality* of endotoxin. Structural analyses thus far have indicated that all the PTSAgs have similar folds.

SPEA is the PTSAg most often associated with streptococcal TSS (Musser et al., 1991). It is a secreted protein with a molecular weight of ~25,000 after removal of its signal peptide. SPEA shares 50–66% primary sequence similarity with SEB and SEC. This high homology has led to the hypothesis that group A streptococci acquired the gene for SPEA from a bacteriophage from *S. aureus* (Betley et al., 1992).

Here, we report the structural analysis of SPEA crystallized in the presence of 10 mM $CdCl_2$. This additive was used because MHC-binding by PTSAgs is frequently dependent upon zinc (Fraser et al., 1992; Abrahmsén et al., 1995; Hudson et al., 1995) and because SEC2 (Papageorgiou et al., 1995) and SEC3 (Hoffmann et al., 1994; Fields et al., 1996) contain zinc-binding sites. Cadmium was chosen over zinc because of its higher electron density. Zinc and cadmium can frequently replace each other. For example,

Reprint requests to: Douglas H. Ohlendorf, University of Minnesota Medical School, Department of Biochemistry, 6-155 Jackson Hall, 321 Church Street, SE, Minneapolis, Minnesota 55455; e-mail: ohlen@dcdiff.med.umn.edu.

Schad et al. (1995) in their structural analysis of SEA located the zinc-binding site using cadmium. Three crystal forms of SPEA were obtained in space groups $P2_12_12_1$, $P2_12_12$, and $P3_121$ (see Table 1). The structure of the first ($P2_12_12_1$) crystal form has been refined to 1.9 Å resolution. Papageorgiou et al. (1999) recently reported the structure of SPEA in the second ($P2_12_12$) crystal form to 2.6 Å resolution in the absence of divalent cations. In a Note Added in Proof, those investigators reported that soaking crystals in an unspecified zinc solution results in metal binding at a site homologous to that found in the SECs. Our results expand these studies by increased resolution of the structures and show that (1) the site homologous to the zinc site in the SECs binds zinc but not cadmium; (2) this site has four endogenous ligands (not three as in the SECs or as reported by Papageorgiou et al., 1995); and (3) cadmium can form a novel cluster that stabilizes the SPEA tetramer.

Materials and methods: *Protein purification:* SPEA was prepared from cultures of group A streptococcal strain 594 grown to stationary phase in a dialyzable beef heart medium. Toxin was purified by ethanol precipitation, resolubilization in pH 4 acetate-buffered saline (5 mM sodium acetate, 150 mM NaCl) and successive preparative thin layer isoelectric focusing in pH gradients of 3 to 10 and then 4 to 6. Ampholytes were removed by dialysis for 4 days against distilled water. Approximately 1.5 mg of SPEA was obtained per liter of culture fluid.

Crystallization of SPEA: Crystals of SPEA were obtained using the hanging drop method. Two microliter aliquots of 10 mg/mL of toxin in 20 mM HEPES, pH 7.5 were mixed with 2 μL of well solution containing 0.25–1.0 M LiCl, 5–20 mM $CdCl_2$, 4–20% PEG 8000, 50 mM Na acetate, pH 3–7. After incubation at 18 °C crystals were obtained. All three crystal forms were obtained under similar conditions.

Diffraction data were collected in house at room temperature using a Bruker-Siemens High Star area detector mounted on a Rigaku RU200 rotating anode generator producing monochromatized Cu-Kα radiation. These data were scaled and merged using the program XENGEN (Howard et al., 1987). Diffraction data were also collected at 77 K using $\lambda = 1.034$ Å radiation produced at beamline 19ID at the Advanced Photon Source at Argonne National Laboratory. These data were scaled and merged using the program DENZO (Otwinowsky & Minor, 1993). Data collection and processing statistics are summarized in Table 1.

Structure solution and refinement: The structure of the $P2_12_12_1$ crystal form was solved by molecular replacement with the program X-PLOR (Brünger, 1993) using the structure of SEC3 (Hoffmann et al., 1994) as a probe. X-PLOR and CNS (Brünger et al., 1998) were used to refine the structural models. Five percent of the data were set aside to assess the progress of refinement using the free *R* value (Brünger, 1992). Model quality was monitored using PROCHECK (Laskowski et al., 1993).

Table 1. *Data processing and refinement*

Data processing				
Space group	$P2_12_12_1$[a]	$P2_12_12_1$	$P2_12_12$	$P3_121$
Unit cell axes (Å)	$a = 55.3$, $b = 126.8$, $c = 148.4$	$a = 55.0$, $b = 126.3$, $c = 147.1$	$a = 105.6$, $b = 130.1$, $c = 84.5$	$a = b = 226.2$, $c = 81.6$
Resolution	1.94 Å	3.0 Å	3.6 Å	3.9 Å
Wavelength	1.0343 Å	1.5405 Å	1.5405 Å	1.5405 Å
Unique reflections	74,721	14,387	12,548	18,614
Completeness	92%	68%	88%	83%
$\langle I/\sigma \rangle$	10.0	7.9	4.0	3.9
R_{sym}	0.062	0.127	0.123	0.119
Molecules in asymmetric unit	4	4	4	8
Refinement				
Protein atoms	7,287	7,292	7,292	14,584
Solvent molecules	626	160	0	0
Cadmium cations	15	15	16	32
Zinc cations	0	4	0	0
Limits on *F*	$F > 1\sigma$	$F > 0$	$F > 0$	$F > 0$
R factor	0.223	0.226	0.232	0.213
Free *R*	0.281	0.295	0.304	0.305
RMS deviation from ideality				
Bond lengths (Å)	0.026	0.010	0.009	0.008
Bond angles (deg)	2.5	1.6	1.5	1.5
Ramachandran plot				
Most-favored region (%)	86.9	79.5	76.7	73.8
Additionally allowed (%)	12.7	19.2	21.8	24.0
Generously allowed (%)	0.4	1.2	1.5	2.2
Disallowed (%)	0.0	0.0	0.0	0.0

[a]Data collected at the Structural Biology Center at the Advanced Photon Source.

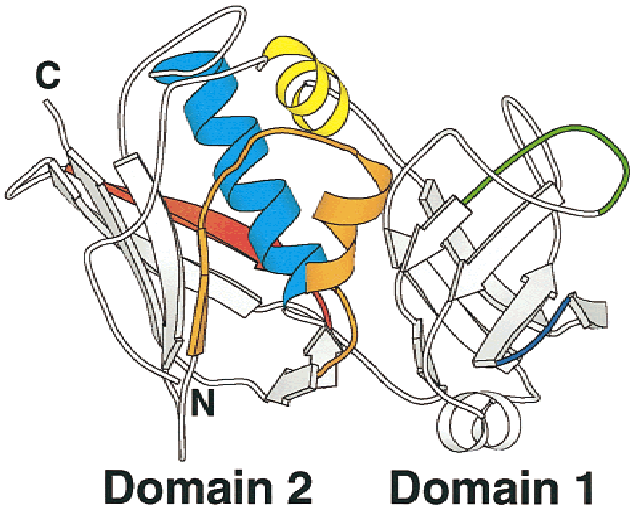

Fig. 1. Ribbon drawing of SPEA. The amino terminal helix is yellow, the $\beta1'$–$\beta2$ loop is blue, the $\beta4$–$\beta5$ loop (disulfide loop) is green, the front flap is orange, the rear flap is red, and the central α-helix is cyan.

The structures of the $P2_12_12$ and $P3_121$ crystal forms were solved by molecular replacement using a partially refined model from the $P2_12_12_1$ crystal form as a structural probe. Because of the reduced resolution of these crystal forms, the structures were only refined by simulated annealing using tight noncrystallographic symmetry restraints. Again, 5% of the diffraction data for each crystal form were set aside for the free *R* value.

Results and discussion: *SPEA monomer:* The final structural model of the SPEA tetramer in the $P2_12_12_1$ crystal form contains 7,287 protein atoms, 626 solvent molecules, and 15 cadmium cations. The side chain of Lys221 has its occupancy set to zero. The main-chain torsion angles for all residues are in the most favored or additionally allowed regions of the Ramachandran plot with the exception of Asn178A, Leu86C, and Leu129D[1] which are in the generously allowed region.

The overall fold of SPEA (see Fig. 1) is typical of the PTSAgs. There are two structural domains. The smaller amino terminal domain (Domain 1) contains five β-strands in a barrel (the first β-strand is split into 2 segments, i.e., $\beta1$ and $\beta1'$). This folding motif known as the OB-fold (Murzin, 1993) is found in several other proteins including staphylococcal nuclease and the B subunits of AB_5 toxins, e.g., cholera toxin. The loop (blue in Fig. 1) between strands $\beta1'$ and $\beta2$ is really two linked turns (type VIII and I) as is found in the other PTSAgs except TSST-1 and SPEC. The loop between strands $\beta3$ and $\beta4$ at the base of the barrel forms an 8-residue α-helix. All the other PTSAgs also have a similar barrel helix except for SPEC, which has only a 4-residue helix (Roussel et al., 1997), and TSST-1, which has no helix (Prasad et al., 1993; Acharya et al., 1994). The loop (green in Fig. 1) between strands $\beta4$ and $\beta5$ contains a disulfide bridge between Cys87 and Cys98. Such disulfide loops are found in all staphylococcal PTSAgs except SEI, SEK, SEL, and TSST-1. Among the streptococcal PTSAgs only SPEA and SSA have disulfide loops.

The larger carboxyl terminal domain (Domain 2) has a 4-turn α-helix resting against a three-strand β-sheet. This folding motif is known as a the β-grasp and has been observed in a number of proteins from bacteria and eukaryotes (Overington, 1992). The central α-helix (cyan in Fig. 1) is nearly entirely covered in front (descriptors such as front, back, and top refer to the orientation presented in Fig. 1) by a flap (orange in Fig. 1) containing a β-strand and an 8-residue helix similar to all other PTSAgs except TSST-1. The first turn of the central α-helix is covered in back by a flap (red in Fig. 1) containing two short β-strands as in all the other PTSAgs except TSST-1 (Prasad et al., 1993; Acharya et al., 1994). The first dozen residues of SPEA form an extended loop against the β-sheet of the β-grasp motif. This loop complete with its single turn of 3_{10} helix is the same as that seen in all other PTSAgs except TSST-1 and SEA. For TSST-1 the amino terminus is truncated. For SEA the helical loop is replaced by a 6-residue helix.

Structural superpositions of the homologous portions of the PTSAgs indicate that SPEA is most similar to SEC2, SEC3, and SEB (root-mean-square (RMS) differences of 0.92, 0.97, and 0.98 Å over 218, 215, and 216 Cαs, respectively). The strong structural homology is consistent with the >40% pairwise sequence identities among these PTSAgs and SEG (Betley et al., 1992) and supports a recent genetic divergence of these toxins. Since these molecules are from different genera, the ancestral toxin was probably transmitted by a phage. The PTSAg with the least homology to SPEA is TSST-1 (22%). As the relative orientation of the two domains TSST-1 have rotated 15°, as compared with SPEA, a superposition was also made allowing for these differences. Even with this adjustment, the RMS difference over 133 Cαs is 1.73 Å for TSST-1.

SPEA tetramer: SPEA monomers associate to form a tetramer with local *222* symmetry (see Fig. 2). The overall shape of the tetramer is like the letter "X" with each bar nearly 90 Å long and 30 Å wide. The bars intersect at a 75° angle; the thickness of the

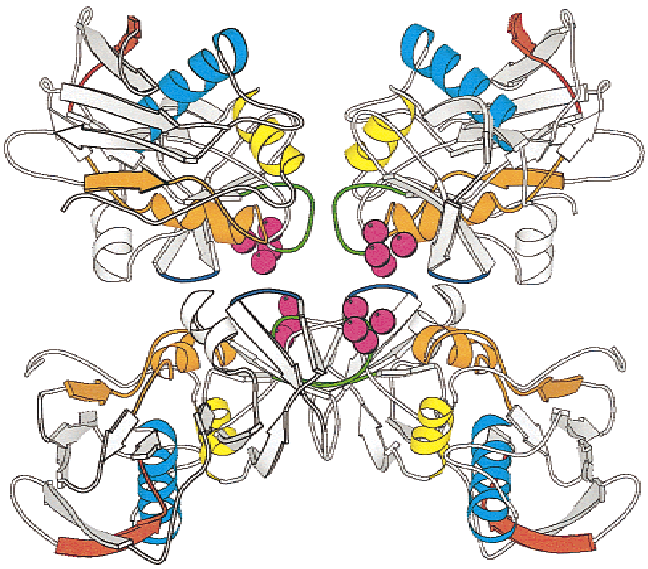

Fig. 2. Ribbon drawing of four monomers in SPEA tetramer. The cadmium clusters are shown as magenta spheres; other colors are as in Figure 1. In the view presented, one twofold axis is vertical in the plane of the paper while another twofold axis is 20° off the viewing axis.

[1]Letters A, B, C, and D are used to denote specific monomers.

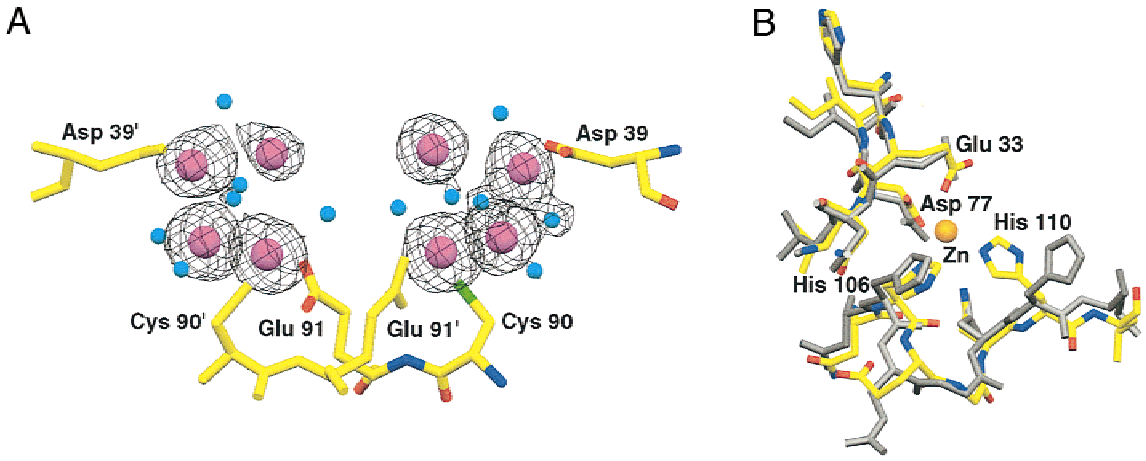

Fig. 3. Metal sites in SPEA. **A:** $+3\sigma F_o - F_c$ map in which the cadmium-solvent clusters were omitted from a cycle of refinement. The cadmiums are magenta, solvent molecules are cyan, and the oxygen, nitrogen and sulfur atoms of the unprimed monomer are red, blue, and yellow, respectively. **B:** Structure at zinc-binding site in 10 mM $ZnCl_2$ (multicolored) and 10 mM $CdCl_2$ (gray).

tetramer is about 45 Å. The tetramer is formed using residues 40–44 in the $\beta 1'$–$\beta 2$ loop, residues 64–65 in the start of the $\beta 3$–$\beta 4$ loop before the barrel helix, residues 85–86 and 88–96 in the $\beta 4$–$\beta 5$ disulfide loop in Domain 1, and residues 189–195 in the top of the front flap covering the central α-helix in Domain 2.

The tetramer is invariant in all known crystal forms. The RMS differences between all Cαs in the tetramers in the three crystal forms reported here are ~0.8 Å. The description of the tetramer observed by Papageorgiou et al. (1999) ($P2_12_12$ crystal form) is consistent with the tetramer we see. In addition, the similar unit cell parameters for the $P2_12_12$ crystal forms obtained by both groups suggest the crystals are isomorphous despite differences in crystallization conditions. The higher resolution reported by Papageorgiou et al. (1999) is likely a consequence of data collection at a synchrotron source.

Structural and mutational studies of SEB, SEC, SPEA, and TSST1 suggest MHC binding uses the surface on the front of Domain 1. Since this surface is blocked in the SPEA tetramer, tetramer–monomer equilibrium will likely modulate superantigenicity. The ability of factors to stabilize the tetramer could be employed to reduce the ability of SPEA to stimulate T-cell proliferation.

Metal sites: $F_o - F_c$ maps from initial refinement cycles of the $P2_22_12_1$ crystal form, using a model of only protein atoms, had several clusters of 10–33σ features. Putting solvent molecules in the strongest difference features resulted in thermal factors of 2 Å^2 (limit allowed by refinement programs) and yet produced strong positive $F_o - F_c$ features. Since SPEA was crystallized from a mother liquor containing cadmium, the largest difference features were modeled as cadmium cations. In subsequent refinement, positive difference features between the cadmiums were modeled as solvent molecules. Figure 3A shows the $+3\sigma$ difference electron density using the final structural model except for the cadmiums and their bridging ligands. Removal of these atoms increased the *R*-factor of the $P2_22_12_1$ crystal form to 0.29.

The four metal clusters are located near the center of the tetramer (2 on one side and 2 on the other) near local twofold axes (see Fig. 2). The minimum distance between clusters is 6.3 Å. The clusters can be best described a forming a tetrahedron where the average Cd–Cd distance is 4.06 ± 0.22 Å (standard deviations presented are calculated from the distances measured in the four clusters). Above five of the six edges of the tetrahedrons are features that have been interpreted as water molecules. The average distance of these molecules from the cadmiums is 2.65 ± 0.20 Å. Above the sixth edge is the Sγ of Cys90, 2.55 ± 0.03 Å from both cadmiums. Extending off cadmiums at three of the peaks of the tetrahedrons are Glu91′[2] making bidentate interactions with a cadmium (d = 2.42 ± 0.11 Å), Asp39 (d = 2.08 ± 0.23 Å), and a solvent molecule (d = 2.41 ± 0.08 Å). The cluster in monomer D is missing the fourth cadmium. In the cluster in monomer A, the fourth cadmium has a bidentate interaction (d = 3.0 Å) with the terminal carboxylate of Lys225′ of an adjacent tetramer. Several of the bridging water molecules have very low thermal parameters and might be chloride anions. The presence of such anions would help neutralize the +8 charge from the cadmiums.

The primary motivation for solving the crystal structures of the $P2_12_12$ and $P3_121$ crystal forms was to discover whether the metal clusters were present in these crystal forms. In both of these crystal forms, a structural model using only protein atoms, produced large difference features (11–15σ for $P2_12_12$ and 4–11σ for $P3_121$ crystal form) overlaying the sites of the metal clusters found in the $P2_12_12_1$ crystal form. For this reason, clusters identical in structure to those found in the $P2_12_12_1$ crystal form were added to the structural models for the lower resolution crystal forms.

The metal cluster found in SPEA is unique. The only clusters resembling those in SPEA are the Fe_4S_4 clusters found in a number of enzymes that catalyze oxidation-reduction reactions (see Beinert et al., 1997 for a review). In those proteins, the four iron and four sulfur atoms form the corners of a cube; the four irons are the corners of a tetrahedron. However, in the Fe_4S_4 clusters the metal–metal distances are somewhat shorter (3.6 Å vs. 4.1 Å) as are the metal-bridging-atom distances (2.3 Å vs. 2.6 Å). In the structure of metallothionein, the cadmium and zinc cations are clustered into

[2]The prime indicates a symmetry-related residue.

cuboidal clusters like those found in Fe_4S_4 clusters (Robbins et al., 1991).

Despite the location of the cluster near the local symmetry axis and the participation of a second monomer in ligating the metals, metal binding is not required for tetramer formation. This conclusion is deduced from the ability of SPEA to crystallize in the $P2_12_12$ crystal form in the absence of cadmium (Papageorgiou et al., 1999).

Papageorgiou et al. (1999) reported in a Note Added in Proof that soaking crystals in zinc solutions results in metal binding at a site homologous to the zinc-binding site reported for SEC2 (Papageorgiou et al., 1995) and SEC3 (Hoffmann et al., 1994). This site is on the back of Domain 1 near its final short β-strand. The electron density maps from crystals grown in 10 mM $CdCl_2$ clearly shows that the side chain of His110 in SPEA has been rotated 116° relative to the conformation of the homologous histidine in SEC2 and no electron density for a cadmium at this site. Soaking crystals for 4 h in 10 mM $ZnCl_2$ in addition to the $CdCl_2$ already in the mother liquor unexpectedly resulted in $+5\sigma$ difference features at the position homologous to the zinc reported in SEC2 and SEC3. Moreover, the difference map indicates that the His110 side chain rotates to a position where it can bind the zinc (see Fig. 3b). At the same time, the Cα of Glu107 moves 1.3 Å away from the zinc. The zinc has four ligands—Glu33, Asp77, His106, and His110—unlike in SEC2 and SEC3 where there zinc has only three ligands.

Acknowledgments: This work has been partially supported by grants from the National Institutes of Health (HL-36611 to P.M.S., GM-54384 to D.H.O.). Greg Vath was partially supported by a National Institute of Health Biophysics training grant (GM 08277). The authors would also like to thank Dr. Tom Poulos for helpful discussions, the Minnesota Supercomputer Institute for the use of computational facilities, the Structural Biology Center at the Advanced Photon Source at Argonne National Laboratory for collection of the $P2_12_12_1$ diffraction data, and Mr. Ed Hoeffner for maintaining the diffraction facilities at the University of Minnesota.

Coordinates for the structural models of the $P2_12_12_1$, $P2_12_12$, and $P3_121$ crystal forms have been deposited in the Protein Data Bank with ID codes 1FNU, 1FNV, and 1FNW, respectively.

References

Abrahmsén L, Dohlsten M, Segren S, Björk P, Jonsson E, Kalland T. 1995. Characterization of two distinct MHC class II binding sites in the superantigen staphylococcal enterotoxin A. *EMBO J 14*:2978–2986.

Acharya KR, Passalacqua EF, Jones EY, Harlos K, Stuart DI, Brehm RD, Tranter HS. 1994. Structural basis of superantigen action inferred from crystal structure of toxic-shock syndrome toxin-1. *Nature 367*:94–97.

Beinert H, Holm RH, Münck E. 1997. Iron-sulfur clusters: Nature's modular, multipurpose structures. *Science 277*:653–659.

Betley MJ, Borst DW, Regassa LB. 1992. Staphylococcal enterotoxins, toxic shock syndrome toxin and streptococcal pyrogenic exotoxins: A comparative study of their molecular biology. *Chem Immunol 55*:1–35.

Brünger AT. 1992. Free *R* value: A novel statistical quantity for assessing the accuracy of crystal structures. *Acta Crystallogr D 49*:24–46.

Brünger AT. 1993. *X-PLOR version 3.1 manual*. New Haven, CT: Yale University.

Brünger AT, Adams PD, Clore GM, DeLano WL, Gros P, Grosse-Kunstleve RW, Jiang JS, Kuszewski J, Nilges M, Pannu NS, et al. 1998. Crystallography & NMR system: A new software suite for macromolecular structure determination. *Acta Crystallogr D 54*:905–921.

Fields BA, Malchiodi EL, Li H, Ysern X, Stauffacher CV, Schlievert PM, Karjalainen K, Mariuzza RA. 1996. Crystal structure of a T-cell receptor β-chain complexed with a superantigen. *Nature 384*:188–192.

Fraser JD, Urban RG, Strominger JL, Robinson H. 1992. Zinc regulates the function of two superantigens. *Proc Natl Acad Sci USA 89*:5507–5511.

Hoffmann ML, Jablonski LM, Crum KK, Hackett SP, Chi YI, Stauffacher CV, Stevens DL, Bohach GA. 1994. Predictions of T-cell receptor- and major histocompatibility complex-binding sites on staphylococcal enterotoxin C1. *Infect Immun 62*:3396–6407.

Howard AJ, Gilliland GL, Finzel BC, Poulos TL, Ohlendorf DH, Salemme FR. 1987. Use of an imaging proportional counter in macromolecular crystallography. *J Appl Crystallogr 20*:383–387.

Hudson KR, Tiedemann RE, Urban RG, Lowe SC, Strominger JL, Fraser JD. 1995. Staphylococcal enterotoxin A has two cooperative binding sites on major histocompatibility complex class II. *J Exp Med 182*:711–720.

Laskowski RA, MacArthur MW, Moss DS, Thornton JM. 1993. PROCHECK: A program to check the stereochemical quality of protein structures. *J Appl Crystallogr 26*:283–291.

Murzin AG. 1993. OB(oligonucleotide/oligosaccharide binding)-fold: Common structural and functional solution for non-homologous sequences. *EMBO J 12*:861–867.

Musser JM, Hauser AR, Kim MH, Schlievert PM, Nelson K, Selander RK. 1991. *Streptococcus pyogenes* causing toxic-shock-like syndrome and other invasive diseases: Clonal diversity and pyrogenic exotoxin expression. *Proc Natl Acad Sci USA 88*:2668–2672.

Otwinowsky Z, Minor W. 1993. *DENZO: A film processing program for macromolecular crystallography*. New Haven, CT: Yale University.

Overington JP. 1992. Comparison of three-dimensional structures of homologous proteins. *Curr Opin Struct Biol 2*:394–401.

Papageorgiou AC, Acharya KR, Shapiro R, Passalacqua EF, Brehm RD, Tranter HS. 1995. Crystal structure of the superantigen enterotoxin C2 from *Staphylococcus aureus* reveals a zinc-binding site. *Structure 3*:769–779.

Papageorgiou AC, Collins CM, Gutman DM, Kline JB, O'Brien SM, Tranter HS, Acharya KR. 1999. Structural basis for the recognition of superantigen streptococcal pyrogenic exotoxin A (SpeA1) by MHC class II molecules and T-cell receptors. *EMBO J 18*:9–21.

Prasad GS, Earhart CA, Murray DL, Novick RP, Schlievert PM, Ohlendorf DH. 1993. Structure of toxic shock syndrome toxin 1. *Biochemistry 32*:13761–13766.

Robbins AH, McRee DE, Williamson M, Collett SA, Xuong NH, Furey WF, Wang BC, Stout CD. 1991. Refined crystal structure of Cd, Zn metallothionein at 2.0 A resolution. *J Mol Biol 221*:1269–1293.

Roussel A, Anderson BF, Baker HM, Fraser JD, Baker EN. 1997. Crystal structure of the streptococcal superantigen SPE-C: Dimerization and zinc binding suggest a novel mode of interaction with MHC class II molecules. *Nat Struct Biol 4*:635–643.

Schad EM, Zaitseva I, Zaitsev VN, Dohlsten M, Kalland T, Schlievert PM, Ohlendorf DH, Svensson LA. 1995. Crystal structure of the superantigen staphylococcal enterotoxin type A. *EMBO J 14*:3292–3301.